This paper is published as part of a *Dalton Transactions* theme issue on:

Nanomaterials for alternative energy sources

Guest editor: Andrew Barron
Rice University, Houston, Texas, USA

Published in issue 40, 2008 of *Dalton Transactions*

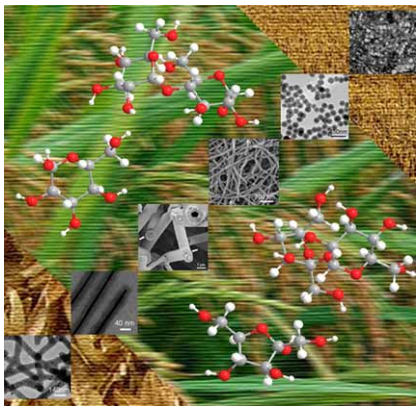

Image reproduced by permission of Shu-Hong Yu

Other papers published in this issue include:

Nanostructured thin solid oxide fuel cells with high power density
Alex Ignatiev, Xin Chen, Naijuan Wu, Zigui Lu and Laverne Smith, *Dalton Trans.,* 2008, DOI: 10.1039/b805658g

Inorganic nanomaterials for batteries
M. Stanley Whittingham, *Dalton Trans.,* 2008, DOI: 10.1039/b806372a

Raman spectroscopy of charge transfer interactions between single wall carbon nanotubes and [FeFe] hydrogenase
Jeffrey L. Blackburn, Drazenka Svedruzic, Timothy J. McDonald, Yong-Hyun Kim, Paul W. King and Michael J. Heben, *Dalton Trans.,* 2008, DOI: 10.1039/b806379f

Shape control of inorganic materials *via* electrodeposition
Kyoung-Shin Choi, *Dalton Trans.*, 2008, DOI: 10.1039/b807848c

Visit the *Dalton Transactions* website for more cutting-edge inorganic materials research
www.rsc.org/dalton

Synthesis of sterically hindered phthalocyanines and their applications to dye-sensitized solar cells

Seunghun Eu,[a] Takashi Katoh,[b] Tomokazu Umeyama,[a] Yoshihiro Matano[a] and Hiroshi Imahori*[a,c,d]

Received 27th February 2008, Accepted 16th May 2008
First published as an Advance Article on the web 30th June 2008
DOI: 10.1039/b803272f

Phthalocyanines with high peripheral substitutions and free from potential contamination by regioisomers have been synthesized and evaluated as photosensitizers for dye-sensitized solar cell applications. Each of the sterically hindered precursor compounds was accomplished by Suzuki–Miyaura cross-coupling reactions with the arylchloride and corresponding boronic acids. Metal free phthalocyanine-sensitized solar cells showed no photocurrent generation due to its low excited singlet state (LUMO) compared with the conduction band of TiO_2. Upon zinc metalation, the LUMO level of the phthalocyanine was pushed up, and this variation afforded an exergonic free energy change for electron injection. The zinc phthalocyanine-sensitized solar cell displayed 0.57% power conversion efficiency (η) and 4.9% maximal IPCE in the near infrared region. More importantly, the cell prepared with and without the presence of chenodeoxycholic acid revealed no difference in the power conversion efficiency. This implies that the well-known aggregation tendency of phthalocyanines that is considered to enhance the self-quenching of the phthalocyanine excited singlet state is effectively suppressed by the high degree of substitutions. The significance of the driving force for electron injection and the distance between the dye core and the TiO_2 surface is also highlighted for devising high performance phthalocyanine photosensitizers.

Introduction

Exhaustion of fossil fuels and global energy concerns have never been recognized as seriously as in recent times. In this context, research activities to acquire energy from the sun, as a clean and inexhaustible resource, are being extensively exploited.[1] After the seminal report of O'Regan and Grätzel,[2] dye-sensitized solar cells (DSSCs) with mesoporous TiO_2 have been regarded as one of the most promising candidates among a variety of regenerative energy sources developed to date. The fundamental aspects of the DSSCs have been well documented based on widespread research efforts to disclose the nature of the devices including interfacial photoinduced electron transfer, role of mesoporous semiconductor electrode, and electrolyte.[3] From the practical and industrial point of view, however, the improvement in the performance has been rather stagnated during the last two decades. The main reason for this could be attributed to the limited light-harvesting capabilities of the existing dyes, especially for the near-infrared region.[4] As such, to devise and develop novel photosensitizer dyes that can effectively harvest red light is an urgent task to make DSSCs practically viable.

Phathalocyanines are the proper choice for this objective due to their strong Q band light absorption properties at around 700 nm.[5] Their extreme stabilities against thermal, chemical, and photochemical reactions are definitively desirable features for the long-term and outdoor robustness of DSSCs. Applications of phthalocyanines for DSSCs as photosensitizers, however, have not been successful.[6] Notoriously poor solubility in common organic solvents and a high tendency to form aggregations have been attributed as the main reasons impeding the revelation of their potential as use for DSSCs. Recent studies by Torres *et al.* and Nazeeruddin *et al.* demonstrated the usefulness of phthalocyanines for red light-harvesting provided that the degree of aggregation is partially diminished by introducing three bulky *t*-butyl groups into the macrocycle plane.[7] The directionality in the excited state of the dye was also emphasized as an important factor for efficient light-harvesting. However, the reported compound is a mixture of regioisomers, and this may result in the formation of rather complex monolayers on the TiO_2 surface, making it difficult to disclose the relationship between the monolayer structure and the photovoltaic properties. More importantly, the cell performance is still aided with the co-adsorption of chenodeoxycholic acid which is well-known to suppress dye aggregation on the TiO_2 surface. Although the power conversion efficiency is the highest among the reported phthalocyanine-sensitized TiO_2 cells (η = 3.5%), it is much lower than those of Ru dye-based DSSCs (η = 10–11%).[2–4] Therefore, further studies are still needed to elucidate the close relationship between molecular structure and photovoltaic properties toward the improvement of cell performance.

Herein we report the synthesis and photovoltaic properties of a novel highly substituted zinc phthalocyanine carboxylic acid (ZnPc) and its metal free counterpart (H_2Pc) as depicted in Fig. 1. The compounds retain eight sterically hindered phenyl groups where the neighboring phenyl rings are rotated about each

[a]*Department of Molecular Engineering, Graduate School of Engineering, Kyoto University, Nishikyo-ku, Kyoto, 615-8510, Japan*
[b]*Goi Research Center, Chisso Petrochemical Corporation, 5-1 Goikaigan, Ichihara, Chiba, 290-8551, Japan*
[c]*Institute for Integrated Cell-Material Sciences (iCeMS), Kyoto University, Nishikyo-ku, Kyoto, 615-8510, Japan*
[d]*Fukui Institute for Fundamental Chemistry, Kyoto University, 34-4, Takano-Nishihiraki-cho, Sakyo-ku, Kyoto, 606-8103, Japan. E-mail: imahori@scl.kyoto-u.ac.jp*

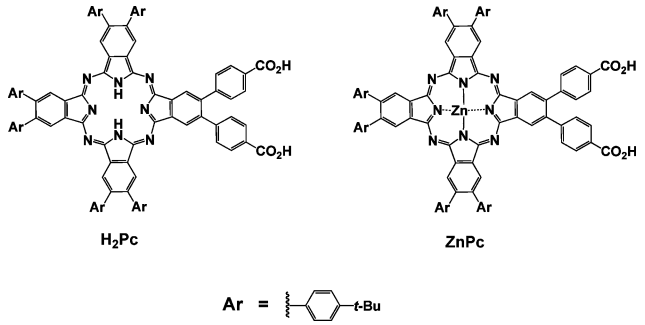

Fig. 1 Structures of the phthalocyanines used in this study.

other with respect to the phthalocyanine plane to avoid steric congestion around the *ortho*-protons. Moreover, the six phenyl groups also possess bulky *t*-butyl moieties. Therefore, ZnPc and H_2Pc are expected to show high solubility toward common organic solvents and a reduced tendency towards aggregation. Since the two neighboring β positions are occupied by the same functional groups, the target compound can be isolated free from the problem of regioisomeric mixtures. Two carboxylic acid binding groups could guarantee stable immobilization of the phthalocyanine onto the TiO_2 surface. Additionally, the intramolecular push–pull character afforded by electron-donating (*t*-butyl) and electron-withdrawing (carboxylic acid) groups would be anticipated to make efficient electron transfer from the phthalocyanine excited singlet state to the conduction band (CB) of the TiO_2.

Results and discussion

Synthesis

The syntheses of the phthalocyanines used in this study were achieved by the statistical condensation method.[8] A key step in this protocol is the preparation of adequate phthalonitrile precursors. Synthetic routes to H_2Pc and ZnPc are displayed in Scheme 1. Precursor compound **1** was accomplished by the Suzuki–Miyaura cross-coupling reaction between 4,5-dichlorophthalonitrile and 4-*t*-butylphenylboronic acid. Suzuki–Miyaura coupling is one of the most widely used reactions for C–C bond formation.[9] However, it is well known that the coupling reactions for substrates with high steric hindrance or for the arylchlorides are ineffective, as for the substrate in this study. To attain the desired compound, we have employed the electron-rich and sterically hindered ligand, 2-(2′,6′-dimethoxybiphenyl)dicyclohexylphosphine (S-Phos).[10]

Because electron-rich ligands with high steric hindrance such as S-Phos or P(*t*-Bu)$_3$ make the palladium(0) coordinatively unsaturated, the cross-coupling reactions even for difficult substrates proceeded smoothly with moderate to good yield.[11] Precursor compound **2** was also achieved through Suzuki–Miyaura cross-coupling between 4,5-dichlorophthalonitrile and 4-(methoxycarbonylphenyl)boronic acid, but it needed longer reaction times compared with that of **1**. Owing to the presence of the ester group, the boronic acid would be an inferior nucleophile compared with 4-*t*-butylphenylboronic acid, and this could be the reason for the longer reaction time.

After obtaining the precursor compounds, we have tried to prepare the desired cyclotetramer by statistical condensation of **1** and **2** in 1-pentanol in the presence of DBU (1,8-diazabicyclo[5.4.0]undec-7-ene). Although we expected to obtain 2,3,9,10,16,17-hexakis(4-*t*-butylphenyl)-23,24-bis(4-methoxycarbonylphenyl)phthalocyanine, we obtained a mixture of two phthalocyanine compounds. The compounds showed two molecular ion peaks at 1630.7 and 1686.8 with an intensity ratio of 1 : 3 in the mass spectrum (MALDI-TOF). The peaks correspond to 2,3,9,10,16,17-hexakis(4-*t*-butylphenyl)-23-(4-methoxycarbonylphenyl)-24-(4-pentoxycarbonylphenyl)phthalocyanine, and 2,3,9,10,16,17-hexakis(4-*t*-butylphenyl)-23,24-bis(4-pentoxycarbonylphenyl)phthalocyanine, respectively. We believed that the exchange reaction between the acetate and pentanoate occurred during the cyclo-condensation reaction, as already reported.[6g,h] Because both of the compounds would afford the same target compound (*i.e.*, H_2Pc) by hydrolysis, the mixture was directly employed for the next reaction without further purification. The basic hydrolysis of the compounds in THF–methanol containing aqueous potassium hydroxide solution afforded the corresponding phthalocyanine carboxylic acid, H_2Pc. To achieve the zinc phthalocyanine carboxylic acid (ZnPc), zinc(II) was inserted into the core of the phthalocyanine esters by treatment with zinc acetate. The resulting compounds displayed molecular ion peaks at 1692.5 and 1748.6 in the mass spectrum (MALDI-TOF). The peaks correspond to 2,3,9,10,16,17-hexakis(4-*t*-butylphenyl)-23-(4-methoxycarbonylphenyl)-24-(4-pentoxycarbonylphenyl)phthalocyanatozinc(II) and 2,3,9,10,16,17-hexakis-(4-*t*-butylphenyl)-23,24-bis(4-pentoxycarbonylphenyl)phthalocyanatozinc(II), respectively. The basic hydrolysis of the compounds in THF–methanol containing aqueous potassium hydroxide solution afforded the corresponding zinc phthalocyanine carboxylic acid, ZnPc. Structures of all the new compounds were verified by spectroscopic analyses including ^{1}H NMR, ^{13}C NMR, FT-IR, mass spectra, and elemental analyses.

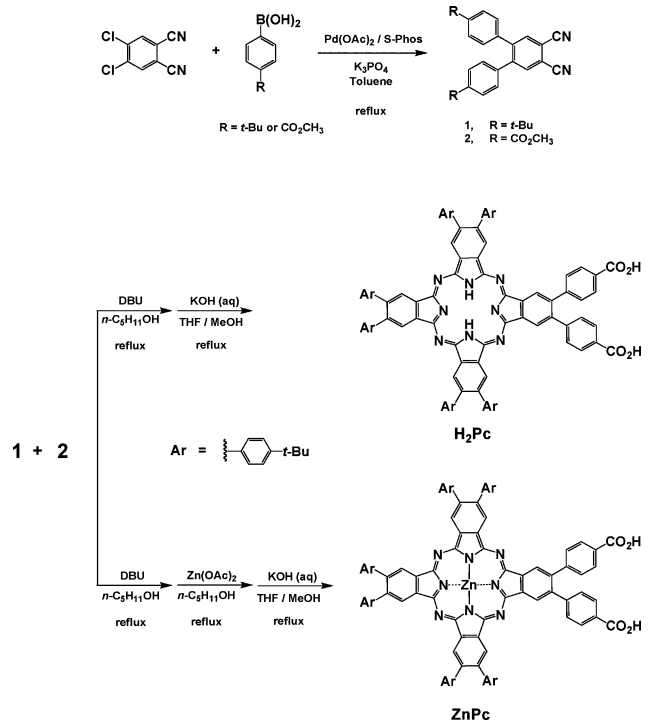

Scheme 1

Optical and electrochemical properties

UV-visible absorption spectra for H_2PC and ZnPc in THF are displayed in Fig. 2. Each of the compounds showed characteristic optical features of zinc and metal free phthalocyanine, respectively. The peak positions in the B and Q band regions are summarized in Table 1. The steady state fluorescence spectra of the phthalocyanines were also measured in THF and the wavelengths for emission maxima are listed in Table 1. The Stokes shifts are determined to be 68.2 cm^{-1} for H_2Pc and 165.6 cm^{-1} for ZnPc. This fairly small value suggests that the variations in the atomic coordinates during the electronic transitions are small for both of the compounds. From the intersection of the normalized absorption and emission spectra, the zero–zero excitation energies ($E_{0\text{-}0}$) are determined to be 1.73 eV for H_2Pc and 1.78 eV for ZnPc in THF.[12]

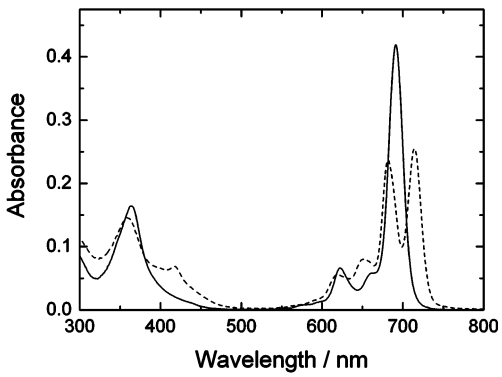

Fig. 2 UV-visible absorption spectra of ZnPc (solid) and H_2Pc (dashed) measured in 2×10^{-6} M of THF solution. Optical length = 1 cm.

To determine the first oxidation potential (E_{ox}) of the phthalocyanines, differential pulse voltammetry (DPV)[13] measurements were performed in DMF containing 0.1 M tetrabutylammonium hexafluorophosphate (TBAP) as a supporting electrolyte and the results are summarized in Table 1. Both H_2Pc and ZnPc display one oxidation peak corresponding to the phthalocyanine radical cation under the same sweep conditions (–0.1 V to +0.8 V *vs* $Ag/AgNO_3$). The oxidation potential of H_2Pc appears at +1.27 V (*vs* NHE), whereas that of ZnPc is determined to be +0.94 V (*vs* NHE). This indicates that the phthalocyanine is easier to oxidize upon zinc(II) metalation, as reported for other phthalocyanine compounds.[14] This variation results in the important consequence of electron injection from the excited state dye (LUMO) to the CB of the TiO_2 (*vide infra*). On the basis of the spectroscopic and electrochemical measurements, driving forces for electron injection from the LUMO of the dye to the CB of the TiO_2 (–0.5 V *vs* NHE) (ΔG_{inj})[15] and the regeneration of the dye radical cation by the I^-/I_3^- redox couple (+0.5 V *vs* NHE) (ΔG_{reg})[15] for the phthalocyanine-sensitized solar cells are evaluated (Table 1). Both of the processes for ZnPc-sensitized TiO_2 cell are thermodynamically feasible, whereas the electron injection from the excited H_2Pc to the CB of the TiO_2 is thermodynamically uphill.

DFT Calculations

DFT calculations were employed to gain insight into the equilibrium geometry and electronic structures for the molecular orbitals of the phthalocyanines. The calculated structures do not show negative frequencies, implying that the optimized geometries are in the global energy minima.[16] Fig. 3 illustrates the electron density distributions of H_2Pc and ZnPc in their respective LUMOs. Sufficient electron densities around the carboxylic acid binding group on the LUMO of the dye are required for good electronic coupling between the excited state of the dye and the 3d orbital of TiO_2.[17] There exists little electron density distribution on and near the carboxylic acid binding groups of the phthalocyanines.

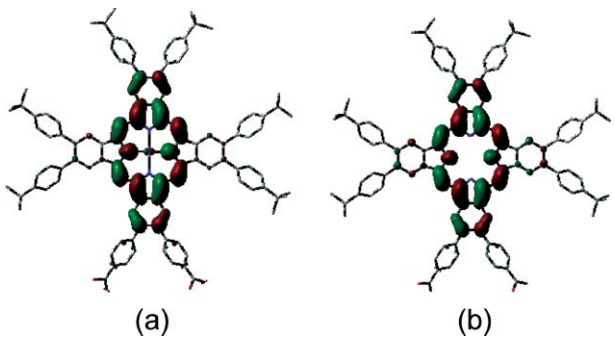

Fig. 3 LUMOs of (a) ZnPc and (b) H_2Pc calculated by DFT methods with B3LYP/3-21G(d). The protons are omitted for clarity.

Table 1 Optical and electrochemical data for the phthalocyanines and driving forces for electron transfer processes on TiO_2

	λ_{abs}[a]/nm	λ_{em}[b]/nm	E_{ox}[c]/V	$E_{0\text{-}0}$[d]/eV	E_{ox}*[e]/V	ΔG_{inj}[f]/eV	ΔG_{reg}[g]/eV
ZnPc	364.5 622.0 691.0	699 730	+0.94	1.78	–0.84	–0.34	–0.44
H_2Pc	357.9, 416.3 619.4, 651.1 681.0, 714.5	718 747	+1.27	1.73	–0.46	+0.04	–0.77

[a] Wavelengths for B and Q band maxima in THF. [b] Wavelengths for emission maxima in THF by exciting at the B band maxima. [c] Ground state oxidation potentials (*vs* NHE). [d] The zero–zero excitation energy estimated from the interaction of the normalized absorption and emission spectra. [e] Excited-state oxidation potentials approximated from E_{ox} and $E_{0\text{-}0}$ (*vs* NHE). [f] Driving forces for electron injection from the phthalocyanine excited singlet state (E_{ox}*) to the conduction band of the TiO_2 (–0.5 V *vs* NHE). [g] Driving forces for the regeneration of phthalocyanine radical cation (E_{ox}) by I^-/I_3^- redox couple (+0.5 V *vs* NHE).

Photovoltaic and photoelectrochemical properties of phthalocyanine-sensitized TiO_2 cells

Mesoporous TiO_2 films (10 μm thick) were prepared from a colloidal suspension of TiO_2 nanoparticles (P25) (see Experimental section). The TiO_2 electrodes were immersed in THF containing 0.05 mM phthalocyanine at room temperature to give the phthalocyanine-modified TiO_2 electrodes. Since the light-harvesting ability and consequently the cell performance are, to a large extent, controlled by surface coverage (Γ) of the dye on the TiO_2 surface, first we examined the immersing time dependency of the Γ value for the phthalocyanines. Both of the dyes showed similar and rather slow adsorption rates, and reached saturated coverage (Γ) on the surface after about 10 h of immersion time (Fig. 4). The total amount of the dyes adsorbed on the TiO_2 surface was determined by measuring the changes in the absorbance of the dye solutions before and after immersing the TiO_2 films. Dye concentrations on the TiO_2 films (0.25 cm^2 of area with thickness of 10 μm) are determined to be about 1.4×10^{-10} mol cm^{-2}. Assuming that (i) the phthalocyanine molecule is a rectangular hexahedron and (ii) the phthalocyanine molecules are densely packed onto the TiO_2 surface with a perpendicular orientation, the occupied area of one molecule on the TiO_2 surface is calculated to be *ca.* 103 $Å^2$ (4.3 × 24.0 $Å^2$). Accordingly, the Γ value is estimated to be 1.6×10^{-10} mol cm^{-2}, which is close to the experimental value. The TiO_2 electrodes modified with H_2Pc and ZnPc are denoted as TiO_2/H_2Pc and TiO_2/ZnPc, respectively.

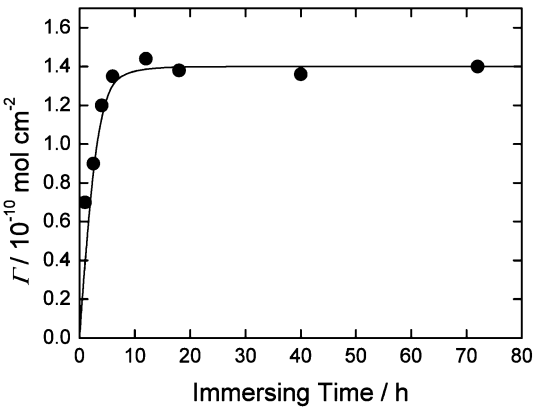

Fig. 4 Profile of the surface coverage (Γ) of ZnPc on the TiO_2 electrode depending on the immersion time of the TiO_2 electrode in a THF solution of ZnPc (0.05 mM).

To judge the potential of H_2Pc and ZnPc as a photosensitizer for DSSC, we evaluated their cell performances using P25 TiO_2 films. A 10 μm thick TiO_2 electrode was modified with H_2Pc (0.05 mM) which was dissolved in THF for an immersion time of 1–72 h. The H_2Pc-sensitized TiO_2 cell showed no power conversion due to the lower energy level of the H_2Pc excited singlet state (–0.46 V *vs* NHE) than that of the CB of the TiO_2 (–0.5 V *vs* NHE).[15] In contrast, the η values of the ZnPc-sensitized cell gradually increased with increasing immersion time to reach maximum η values (η_{max}) of *ca.* 0.6% for 12 h. The power conversion efficiency (η) is derived from the equation: $\eta = J_{SC} \times V_{OC} \times ff$, where J_{SC} is the short circuit current, V_{OC} is the open circuit potential, and *ff* is the fill factor. Further increases of the immersion time of up to 72 h exhibited no noticeable changes in the η values. The time profiles of the η values (Fig. 5) correlate well with those of the Γ values (*vide supra*). This is in sharp contrast with the porphyrin-sensitized TiO_2 cells in which at first the η values increase and then decrease significantly with increasing immersion time.[4b,18] The representative photocurrent–voltage characteristics of ZnPc-sensitized TiO_2 cells with an immersion time of 12 h is depicted in Fig. 6; $\eta = 0.57 \pm 0.03\%$ with $J_{SC} = 1.47 \pm 0.05$ mA cm^{-2}, $V_{OC} = 0.54 \pm 0.02$ V, and $ff = 0.71 \pm 0.03$.

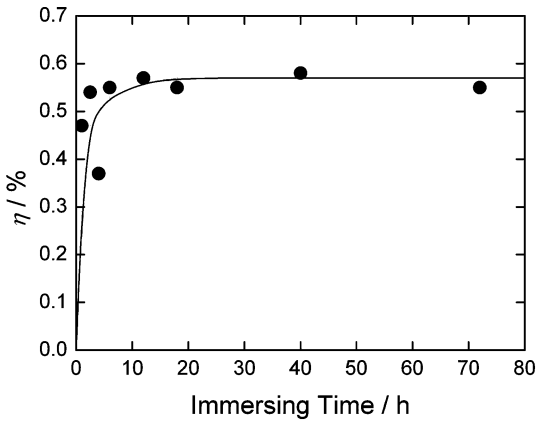

Fig. 5 Profile of the power conversion efficiency (η) of a ZnPc-sensitized TiO_2 cell depending on the immersion time of the TiO_2 electrode in ZnPc–THF solution (0.05 mM).

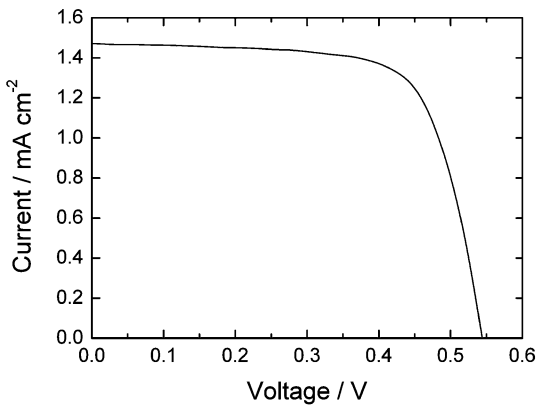

Fig. 6 Photocurrent–voltage characteristics of a ZnPc-sensitized TiO_2 cell ($\eta = 0.57\%$, $J_{sc} = 1.47$ mA cm^{-2}, $V_{oc} = 0.54$ V, $ff = 0.71$). Conditions: electrolyte 0.1 M LiI, 0.05 M I_2, 0.6 M 2,3-dimethyl-1-propyl imidazolium iodide, and 0.5 M 4-*t*-butylpyridine in CH_3CN; input power: AM 1.5 under simulated solar light (100 mW cm^{-2}). $\eta = J_{sc} \times V_{oc} \times ff$.

For the phthalocyanine-sensitized TiO_2 cell, co-adsorbates such as chenodeoxycholic acid have been employed to reduce the tendency of dye aggregation on the TiO_2 surface.[6,7] For instance, in a previous report Sundström *et al.* manufactured double enhanced performance by introducing the co-adsorbates into the immersion bath ($\eta = 0.29\%$ in the absence of the co-adsorbates and $\eta = 0.54\%$ in the presence of the co-adsorbates).[19] To further improve the performance of the present cell, we also introduced chenodeoxychloic acid (2.5 mM) to the ZnPc–THF solution (0.05 mM), and prepared the phthalocyanine-sensitized TiO_2 cell. The cell, however, exhibited no apparent difference in the η values with the cell prepared in the absence of chenodeoxycholic acid under the same conditions (Fig. 7); $\eta = 0.54 \pm 0.03\%$,

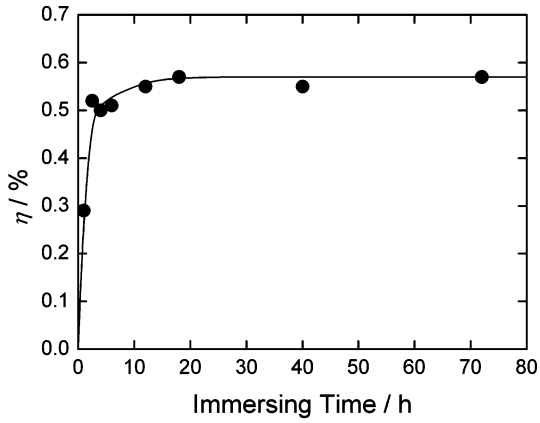

Fig. 7 Profile of the power conversion efficiency (η) of a ZnPc-sensitized TiO_2 cell depending on the immersion time of the TiO_2 electrode in ZnPc–THF solution (0.05 mM) in the presence of chenodeoxycholic acid (2.5 mM).

$J_{sc} = 1.44 \pm 0.06$ mA cm^{-2}, $V_{oc} = 0.54 \pm 0.03$ V, and $ff = 0.70 \pm 0.03$ for the cell with chenodeoxycholic acid. If there exist significant aggregations of ZnPc on the TiO_2 surface, the electron injection yield would be considerably diminished by the accelerated decay of the ZnPc excited singlet state, leading to a fair decrease in the cell performance, especially in the short circuit current. No apparent difference between the two cells with and without the presence of chenodeoxycholic acid reveals that the performance of our present cell is not perturbed by the well-known tendency of phthalocyanine aggregation. We understood this phenomenon to originate from the high steric hindrance of the ZnPc. Considering that the degree of dye aggregation on the TiO_2 surface is generally increased along with prolonged immersion, this interpretation is consistent with the parallel correlation between the time profile of the η values and the Γ values (*vide supra*).

To investigate the photovoltaic response of the present cell in more detail, we measured the photocurrent action spectra of a ZnPc-sensitized TiO_2 cell under the same conditions as for the photocurrent–voltage characteristic measurements (Fig. 8a).[20] To a large extent, the photocurrent response follows the general trend of the absorption feature of ZnPc/TiO_2 (Fig. 8b), indicating that the phthalocyanine is the main source of the photocurrent generation. The maximal IPCE value at the near-infrared region is measured to be 4.9%.

Considering the full coverage of the TiO_2 surface and the high molar extinction coefficient around the 700 nm region for ZnPc, the low IPCE value of the ZnPc-sensitized TiO_2 cell cannot be explained by light-harvesting efficiency. The remaining two factors are the quantum yield of the electron injection from the ZnPc excited singlet state to the CB of the TiO_2 electrode, and the efficiency of charge collection.[21] The charge collection efficiency is determined primarily by the relative rate of charge transport and charge recombination. In DSSCs, the injected electron can be recombined with the resulting dye cation and I^-/I_3^- redox couple before going to the outer circuit.[22] The charge transport is reported to occur on the timescale of 10^{-7}–10^{-5} s, whereas the recombination between the electron and I^-/I_3^- happens on the timescale of 10^{-3}–1 s.[23,24] Although the time scale of the charge recombination with the resulting dye cation is known to vary depending on the electron density on TiO_2, a typical range is from

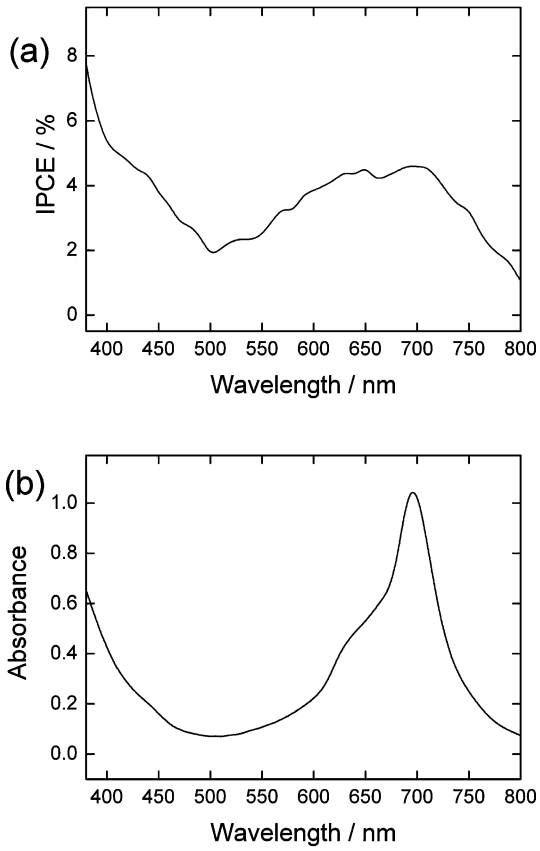

Fig. 8 (a) Photocurrent action spectra of a ZnPc-sensitized TiO_2 cell. The phthalocyanine-modified TiO_2 electrode was prepared under the same conditions as for the power conversion efficiency (η) measurements. Conditions: electrolyte 0.1 M LiI, 0.05 M I_2, 0.6 M 2,3-dimethyl-1-propyl imidazolium iodide, and 0.5 M 4-*t*-butylpyridine in CH_3CN; input power: AM 1.5 under simulated solar light (100 mW cm^{-2}). (b) UV-visible absorption spectra of TiO_2/ZnPc. The thickness of the TiO_2 was adjusted to be 700–1000 nm to obtain the shape and peak position of the spectra accurately.

10^{-5} to 10^{-3} s.[23,25] Therefore, the charge collection efficiency may not be the limiting factor for the low photocurrent generation. The quantum yield of electron injection is controlled by the competing processes against electron injection such as intersystem crossing, nonradiative decay, emission, and excited-state quenching; the most important factor is, however, the driving force for electron injection (ΔG_{inj}) from the excited state dye to the CB of the TiO_2.[3c] From the solution electrochemistry and spectroscopy, the ΔG_{inj} for the ZnPc-sensitized TiO_2 cell is determined to be –0.34 eV. Apparently, it indicates that electron injection is a thermodynamically feasible process. The energy level of the CB is, however, not laid at a fixed point but is subject to change depending on the operating conditions of the DSSCs. Mesoporous TiO_2 films have been known to show Nernstian shifts in their CB level depending on the degree of surface protonation.[26] The shift of the CB of about 0.3 eV related to the changes in the electrolyte composition is also reported.[22] Besides, the level of the CB would be raised to some degree due to the electron injection itself. The oxidation potential of the dye, in addition, is positively shifted by the chemical adsorption on the TiO_2.[18c,27] Thus, the actual driving force for the ZnPc-sensitized cell is estimated to be

smaller than the above-mentioned value. In such a case, electron injection from the excited ZnPc to the CB of the TiO_2 may occur mainly or only through surface states because there exist little available acceptor states for efficient electron injection.[28] Besides, the electronic coupling between the LUMO of the ZnPc and the 3d orbital of the TiO_2 cannot be anticipated to be large enough due to no apparent electron density on the carboxylic acid binding groups together with the intervening phenyl moieties between the ZnPc core and the carboxylic acid (*vide supra*). Thus, both the small driving force and the weak electronic coupling would make ZnPc an inefficient photosensitizer for DSSCs.

Certainly, the performance of our present cell is not good and is far from our expectations. From this study, however, we can detect invaluable clues for devising effective phthalocyanine photosensitizers for DSSC applications.

Conclusions

Sterically hindered zinc phthalocyanine carboxylic acid (ZnPc) and its metal free counterpart (H_2Pc) were synthesized and evaluated as photosensitizers for DSSC applications. The H_2Pc-sensitized TiO_2 cell showed no photocurrent response due to its low excited singlet state compared with the CB of TiO_2. The ZnPc-sensitized TiO_2 cell displayed 0.57% of power conversion efficiency (η) and 4.9% maximal IPCE value in the near-infrared region. Introduction of chenodeoxycholic acid revealed no noticeable change in the cell performance, showing that the aggregation of ZnPc is effectively suppressed by steric hindrance. The moderate cell performance can be rationalized by the small driving force for electron injection from the excited-state ZnPc to TiO_2, and the poor electronic coupling between the LUMO of ZnPc and the CB of TiO_2. Thus, this study affords important basic information for devising novel phthalocyanines for DSSC applications.

Experimental

General

All solvents and chemicals were of reagent grade quality, purchased, and used without further purification unless otherwise noted. Column chromatography and thin-layer chromatography (TLC) were performed with UltraPure Silica Gel (230–400 mesh, SiliCycle) and Silica gel 60 F_{254} (Merck), respectively. ^{1}H NMR spectra were measured on a JEOL EX-400 (400 MHz) or a Varian Unity 500 (500 MHz) spectrometer. ^{13}C NMR spectra were measured on a JEOL EX-400 (100 MHz) spectrometer. High-resolution mass spectra (HRMS) were recorded on a JEOL JMS-HX 110A spectrometer (FAB) using 3-nitrobenzylic alcohol as a matrix or a JEOL JMS-700 MStation spectrometer (EI). Matrix assisted laser desorption/ionization time-of-flight (MALDI-TOF) mass spectra were made on a BRUKER Autoflex III using CHCA (α-cyano-4-hydroxycinnamic acid) as matrix. UV-visible absorption spectra were measured using a Perkin-Elmer Lambda 900 UV/vis/NIR Spectrometer. Steady-state fluorescence spectra were acquired with a SPEX Fluoromax-3 Spectrofluorometer. Spectroscopy grade tetrahydrofuran was used for the measurements of UV-visible absorption and fluorescence spectra. FT-IR spectra were acquired using a JASCO FT/IR-470 plus or a FT/IR-4200 spectrometer with a KBr pellet. Melting points were recorded on a Yanagimoto micro-melting point apparatus and were not corrected.

Electrochemical measurements were made using a BAS 50 W electrochemical workstation. Oxidation potentials in solution were determined by differential pulse voltammetry (DPV) with a pulse amplitude of 50 mV in Ar saturated *N, N′*-dimethylformamide containing 0.1 M tetrabutylammonium perchlorate (TBAP) as supporting electrolyte. A glassy carbon working electrode (3 mm diameter), $Ag/AgNO_3$ reference electrode, and Pt wire counter electrode were employed. Ferrocene/ferrocenium (+0.642 V *vs* NHE) was used as an internal standard for all measurements. The measured potentials were quoted with reference to NHE.

Synthesis

4,5-Bis(4-*t*-butylphenyl)phthalonitrile (1). Although this compound has already been reported, the previous characterization is not complete.[29] A 100 mL round-bottomed flask was charged with 4,5-dichlorophthalonitrile (1.87 g, 9.5 mmol), 4-*t*-butylphenylboronic acid (5.0 g, 28.1 mmol), palladium(II) acetate (44 mg, 0.2 mmol), 2-(2′,6′-dimethoxybiphenyl)dicyclohexylphosphine (200 mg, 0.49 mmol), K_3PO_4 (8.48 g, 40 mmol), and anhydrous toluene (25 mL). The solution was stirred at 90 °C for 2 h. After cooling to room temperature, the reaction mixture was washed twice with water. The combined organic layers were washed once with water, subsequently dried over anhydrous magnesium sulfate, and then concentrated *in vacuo*. The residue was dissolved in hexane, and the solid material was obtained by precipitation. Dissolution in and reprecipitation with cold hexane was repeated until no solid material appeared. Reprecipitation of the combined crude product with ethyl acetate–hexane afforded **1** as needle-like off-white crystals (2.44 g, 6.22 mmol, 66% yield); mp 165.2–166.9 °C; ^{1}H NMR (400 MHz, $CDCl_3$) δ 7.82 (s, 2H, phenyl H), 7.28 (d, J = 8.3 Hz, 4H, phenyl H), 7.03 (d, J = 8.3 Hz, 4H, phenyl H), 1.29 (s, 18H, *t*-butyl H); ^{13}C NMR (100 MHz, $CDCl_3$) δ 151.77, 145.81, 135.54, 134.80, 129.01, 125.46, 115.56, 113.97, 34.64, 31.20; FT-IR (KBr) ν_{max} 2964, 2905, 2869, 2233 (CN), 1735, 1608, 1589, 1484, 1462, 1363, 1268, 1113, 1015, 915, 835, 594, 569 cm^{-1}; HRMS (EI positive) m/z calcd 392.2252 (for $C_{28}H_{28}N_2$), found 392.2249; elemental analysis (% calcd, % found for $C_{28}H_{28}N_2$) : C (85.67, 85.37), H (7.19, 7.30), N (7.14, 6.87).

4,5-Bis(4-methoxycarbonylphenyl)phthalonitrile (2). A 100 mL round-bottomed flask was charged with 4,5-dichlorophthalonitrile (1.0 g, 5.1 mmol), 4-(methoxycarbonylphenyl)-boronic acid (2.7 g, 15.0 mmol), palladium(II) acetate (22 mg, 0.1 mmol), 2-(2′,6′-dimethoxybiphenyl)dicyclohexylphosphine (100 mg, 0.25 mmol), K_3PO_4 (4.24 g, 20 mmol), and anhydrous toluene (20 mL). The solution was stirred at 90 °C for 15 h. After cooling to room temperature, the reaction mixture was washed twice with water. The combined organic layers were washed once with water, subsequently dried over anhydrous magnesium sulfate, and then concentrated *in vacuo*. Reprecipitation of the crude product from ethyl acetate twice afforded **2** as plate-like off-white crystals (1.20 g, 2.62 mmol, 60.6% yield); mp 225.6–227.1 °C; ^{1}H NMR (300 MHz, $CDCl_3$) δ 7.96 (d, J= 8.4 Hz, 4H, phenyl H), 7.89 (s, 2H, phenyl H), 7.17 (d, J = 8.4 Hz, 4H, phenyl H), 3.92 (s, 6H, ester H); ^{13}C NMR (75 MHz, $CDCl_3$) δ 166.20, 144.86, 141.58, 135.39, 130.50, 130.00, 129.39, 115.31, 114.97, 52.38; FT-IR (KBr) ν_{max} 3437, 2236 (CN), 1725, 1609, 1436, 1314,

1282, 1188, 1115, 1105, 1018, 861, 777, 713, 523 cm^{-1}; HRMS (EI positive) m/z calcd 396.1110 (for $C_{26}H_{16}N_2O_4$), found 396.1114; elemental analysis (% calcd, % found for $C_{26}H_{16}N_2O_4$) : C (72.72, 72.79), H (4.07, 4.05), O (16.14, 16.29), N (7.07, 6.87).

2,3,9,10,16,17-Hexakis(4-*t*-butylphenyl)-23,24-bis(4-carboxyphenyl)phthalocyanine (H_2Pc). A 200 mL round-bottomed flask was charged with **1** (4.24 g, 10.8 mmol), **2** (1.43 g, 3.60 mmol), 1,8-diazabicyclo[5.4.0]undec-7-ene (DBU) (0.3 g, 1.97 mmol), and 1-pentanol (60 mL). The solution was stirred at reflux for 20 h and cooled to room temperature. The solvent was then removed under reduced pressure. Solid material was obtained from methanol, and subjected to silica gel column chromatography (chloroform–hexane = 3 : 1). The second fraction was collected and reprecipitated from methanol. Silica gel column chromatography (chloroform–hexane = 1 : 5) of the previously collected material afforded a dark green solid (1.02 g). The solid showed two molecular ion peaks at 1630.7 and 1686.8 with an intensity ratio of 1 : 3 in the mass spectrum (MALDI-TOF). The peaks correspond to 2,3,9,10,16,17-hexakis-(4-*t*-butylphenyl)-23-(4-methoxycarbonylphenyl)-24-(4-pentoxycarbonylphenyl)phthalocyanine, and 2,3,9,10,16,17-hexakis(4-*t*-butylphenyl)-23,24-bis(4-pentoxycarbonylphenyl)phthalocyanine, respectively. The mixture was directly employed for the next reaction without further purification.

To a solution of the previously collected dark green solid (1.03 g) in THF–methanol (2 : 1 (v/v), 280 mL) in a 500 mL round-bottomed flask was added a 40% aqueous KOH solution (40 mL). The solution was stirred at reflux for 8 h, cooled to room temperature, and the organic solvent was removed under reduced pressure. The pH of the reaction mixture was set to 2 by adding HCl solution (6 M), and a precipitate was formed. The precipitate was collected and washed with copious amounts of water and dried. The collected solid material was suspended in chloroform (100 mL), and stirred at reflux for 1 h. Filtering, and subsequent drying under reduced pressure of the solid afforded H_2Pc as a dark green solid (336 mg, 6.0% overall yield for 2 steps with reference to **2** used); mp > 300 °C; ^{1}H NMR (400 MHz, THF-d_8) δ 10.83 (s, 1H, carboxy H), 9.18 (s, 6H, phenyl H (2,3,9,10,16,17)), 9.15 (s, 2H, phenyl H (23,24)), 8.08 (d, 4H, J = 8.3 Hz, carboxyphenyl H), 7.63 (d, 4H, J = 8.3 Hz, carboxyphenyl H), 7.49 (d, 4H, J = 8.3 Hz, carboxyphenyl H), 7.43 (s, 20H, carboxyphenyl H), 1.43 (s, 36H, *t*-Bu H), 1.41 (s, 18H, *t*-Bu H), −1.55 (br s, 2H, inner H); FT-IR (KBr) ν_{max} 3431, 3296, 2962, 2903, 1716, 1698, 1609, 1506, 1499, 1446, 1435, 1395, 1363, 1315, 1292, 1269, 1105, 1011, 925, 835, 764, 727, 719 cm^{-1}; HRMS (FAB positive) m/z calcd 1547.7745 (for $C_{106}H_{98}N_8O_4$), found 1547.7822 $(M + H)^+$.

2,3,9,10,16,17-Hexakis(4-*t*-butylphenyl)-23,24-bis(4-carboxyphenyl)phthalocyanatozinc(II) (ZnPc). To a solution of the previously collected dark green solid (500 mg, mixture of the 2,3,9,10,16,17-hexakis(4-*t*-butylphenyl)-23-(4-methoxycarbonylphenyl)-24-(4-pentoxycarbonylphenyl)phthalocyanine and 2,3,9,10,16,17-hexakis(4-*t*-butylphenyl)-23,24-bis(4-pentoxycarbonylphenyl)phthalocyanine) in 1-pentanol (100 mL) in a 300 mL round-bottomed flask was added anhydrous zinc acetate (500 mg, 3.0 mmol). The solution was stirred at 130 °C for 3 h under a nitrogen atmosphere. After cooling to room temperature, the solvent was removed under reduced pressure. Silica gel column chromatography (chloroform) of the crude product afforded a green solid (103 mg). The solid showed two molecular ion peaks at 1692.5 and 1748.6 with an intensity ratio of 1 : 3 in the mass spectrum (MALDI-TOF). The peaks correspond to 2,3,9,10,16,17-hexakis(4-*t*-butylphenyl)-23-(4-methoxycarbonylphenyl) - 24 - (4 - pentoxycarbonylphenyl) phthalocyanatozinc(II), and 2,3,9,10,16,17-hexakis(4-*t*-butylphenyl)-23,24-bis(4-pentoxycarbonylphenyl)phthalocyanatozinc(II), respectively. The mixture was directly employed for the next reaction without further purification.

To a solution of the previously collected green solid (103 mg) in THF–methanol (2 : 1 (v/v), 30 mL) in a 100 mL round-bottomed flask was added a 40% aqueous KOH solution (30 mL). The solution was stirred at reflux for 5 h, cooled to room temperature, and the organic solvent was removed under reduced pressure. The pH of the reaction mixture was set to 4 by adding 6 M HCl solution, and a precipitate was formed. The precipitate was collected and washed with copius amounts of water and dried. The collected solid material was suspended in chloroform (100 mL), and stirred at reflux for 1 h. Filtering, and subsequent drying under reduced pressure of the solid afforded ZnPc as a dark green solid (52.6 mg, 4.6% overall yield for 3 steps with reference to **2** used); mp > 300 °C; ^{1}H NMR (400 MHz, THF-d_8) δ 10.72 (s, 1H, carboxy H), 9.47 (s, 2H, phenyl H (23,24)), 9.40 (s, 2H, phenyl H (9,10)), 9.39 (s, 4H, phenyl H (2,3,16,17)), 8.10 (d, 4H, J = 8.3 Hz, carboxyphenyl H), 7.72 (d, 4H, J = 8.3 Hz, carboxyphenyl H), 7.53 (skewed d, J = 8.3 Hz, 12H, carboxyphenyl H), 7.46 (skewed d, J = 8.3 Hz, 12H, carboxyphenyl H), 1.41 (s, 36H, *t*-Bu H), 1.40 (s, 18H, *t*-Bu H); HRMS (FAB positive) m/z calcd 1608.6846 (for $C_{106}H_{96}N_8O_4Zn$), found 1608.6816 $(M + H)^+$.

Density functional theory (DFT) calculations

Geometry optimization and electronic structure calculations of the phthalocyanines were performed using the B3LYP functional and 3-21G(d) basis set implemented in the Gaussian 03 program package.[30] Molecular orbitals were visualized by GaussView 3.0 software.

Preparation of phthalocyanine-modified TiO_2 electrode and photovoltaic measurements

Preparation of mesoporous TiO_2 films and immobilization of the phthalocyanine on the TiO_2 surface, and characterization of the photovoltaic properties of phthalocyanine-modified TiO_2 were made by following the procedures reported previously.[18] Tetrahydrofuran was used as an immersion solvent in the present experiments instead of ethanol or methanol. The TiO_2 electrodes modified with H_2Pc and ZnPc are denoted as TiO_2/H_2Pc and TiO_2/ZnPc, respectively. The amounts of phthalocyanine adsorbed on the TiO_2 films were determined by measuring the changes in the absorbance of the phthalocyanine solutions (4 mL) before and after immersion of the TiO_2 films (0.25 cm^2 of projected area). All the experimental values were given as an average from six independent measurements.

Acknowledgements

This work was supported by Grant-in-Aid (No. 19350068 for H.I.) from the Ministry of Education, Culture, Sports, Science and Technology (MEXT), Japan and NEDO. We gratefully

acknowledge Prof. Susumu Yoshikawa (Kyoto University) and Prof. Shozo Yanagida and Dr Naruhiko Masaki (Osaka University) for the use of the equipment for photovoltaic measurements. Computation time was provided by the Academic Center for Computing and Media Studies, Kyoto University. S. E. thanks the International Doctoral Program in Engineering, Graduate School of Engineering, Kyoto University, for financial support.

Notes and references

1 (*a*) C. W. Tang, *Appl. Phys. Lett.*, 1986, **48**, 183; (*b*) G. Yu, J. Gao, J. C. Hummelen, F. Wudl and A. J. Heeger, *Science*, 1995, **270**, 1789; (*c*) C. A. Bignozzi, R. Argazzi and C. J. Kleverlaan, *Chem. Soc. Rev.*, 2000, **29**, 87; (*d*) H. Imahori, *J. Mater. Chem.*, 2007, **17**, 31.

2 B. O'Regan and M. Grätzel, *Nature*, 1991, **353**, 737.

3 (*a*) Special issue on dye-sensitized solar cells: *Coord. Chem. Rev.*, 2004, **248**, p. 1161; (*b*) Forum on solar and renewable energy: *Inorg. Chem.*, 2005, **44**, p. 6799; (*c*) D. F. Watson and G. J. Meyer, *Annu. Rev. Phys. Chem.*, 2005, **56**, 119; (*d*) N. A. Anderson and T. Lian, *Annu. Rev. Phys. Chem.*, 2005, **56**, 491; (*e*) W. R. Duncan and O. V. Prezhdo, *Annu. Rev. Phys. Chem.*, 2007, **58**, 143; (*f*) N. Robertson, *Angew. Chem., Int. Ed.*, 2006, **45**, 2338.

4 (*a*) N. Robertson, *Angew. Chem., Int. Ed.*, 2008, **47**, 1012; (*b*) M. Tanaka, S. Hayashi, S. Eu, T. Umeyama, Y. Matano and H. Imahori, *Chem. Commun.*, 2007, 2069; (*c*) Y. Shibano, T. Umeyama, Y. Matano and H. Imahori, *Org. Lett.*, 2007, **9**, 1971.

5 G. de la Torre, C. G. Claessens and T. Torres, *Chem. Commun.*, 2007, 2000.

6 (*a*) Md. K. Nazeeruddin, R. Humphry-Baker, M. Grätzek, D. Wöhrle, S. Schnurpfeil, G. Schneider, A. Hirth and N. Trombach, *J. Porphyrins Phthalocyanines*, 1999, **3**, 230; (*b*) V. Aranyos, J. Hjelm, A. Hagfeldt and H. Grennberg, *J. Porphyrins Phthalocyanines*, 2001, **5**, 609; (*c*) J. He, A. Hagfeldt, S.-E. Lindquist, H. Grennberg, F. Korodi, L. Sun and B. Åkermark, *Langmuir*, 2001, **17**, 2743; (*d*) Y. Amao and T. Komori, *Langmuir*, 2003, **19**, 8872; (*e*) E. Palomares, M. V. Martinez-Diaz, S. A. Haque, T. Torres and J. R. Durrant, *Chem. Commun.*, 2004, 2112; (*f*) L. Giribabu, C. H. V. Kumar, V. G. Reddy, P. Y. Reddy, Ch. S. Rao, S.-R. Jang, J.-H. Yum, Md. K. Nazeeruddin and M. Grätzel, *Sol. Energy Mater. Sol. Cells*, 2007, **91**, 1611; (*g*) M. Yanagisawa, F. Korodi, J. He, L. Sun, V. Sundström and B. Åkermark, *J. Porphyrins Phthalocyanines*, 2002, **6**, 217; (*h*) M. Yanagisawa, F. Korodi, J. Bergquist, A. Holmberg, A. Hagfeldt, B. Åkermark and L. Sun, *J. Porphyrins Phthalocyanines*, 2004, **8**, 1228; (*i*) A. Morandeira, I. Lopez-Duarte, M. V. Martínez-Díaz, B. O'Regan, C. Shuttle, N. A. Haji-Zainulabidin, T. Torres, E. Palomares and J. R. Durrant, *J. Am. Chem. Soc.*, 2007, **129**, 9250; (*j*) B. O'Regan, I. Lopez-Duarte, M. V. Martínez-Díaz, A. Forneli, J. Albero, A. Morandeira, E. Palomares, T. Torres and J. R. Durrant, *J. Am. Chem. Soc.*, 2008, **130**, 2906.

7 (*a*) P. Y. Reddy, L. Giribabu, C. Lyness, H. J. Snaith, C. Vijaykumar, M. Chandrasekharam, M. Lakshmikantam, J.-H. Yum, K. Kalyanasundaram, M. Grätzel and Md. K. Nazeeruddin, *Angew. Chem., Int. Ed.*, 2007, **46**, 373; (*b*) J.-J. Cid, J.-H. Yum, S.-R. Jang, Md. K. Nazeeruddin, E. Martínez-Ferrero, E. Palomares, J. Ko, M. Grätzel and T. Torres, *Angew. Chem., Int. Ed.*, 2007, **46**, 8358.

8 M. S. Rodríguez-Morgade, G. de la Torre and T. Torres, in *The Porphyrin Handbook*, ed. K. M. Kadish, K. M. Smith and R. Guilard, Academic Press, New York, 2000, vol. 15, ch. 99, pp. 125–160.

9 (*a*) N. Miyaura and A. Suzuki, *Chem. Rev.*, 1995, **95**, 2457; (*b*) A. Suzuki, *J. Organomet. Chem.*, 1999, **576**, 147; (*c*) J.-P. Corbet and G. Mignani, *Chem. Rev.*, 2006, **106**, 2651.

10 J. Yin, M. P. Rainka, X.-X. Zhang and S. L. Buchwald, *J. Am. Chem. Soc.*, 2002, **124**, 1162.

11 (*a*) A. F. Littke, C. Dai and G. C. Fu, *J. Am. Chem. Soc.*, 2000, **122**, 4020; (*b*) A. F. Littke, C. Dai and G. C. Fu, *J. Am. Chem. Soc.*, 2002, **124**, 1162; (*c*) S. P. Nolan and O. Navarro, in *Comprehensive Organometallic Chemistry III*, ed. R. H. Crabtree and D. M. P. Mingos, Elsevier, Oxford, 2007, vol. 11, ch. 11.01, p. 7.

12 J. Gierschner, J. Cornil and H.-J. Egelhaaf, *Adv. Mater.*, 2007, **19**, 173.

13 The oxidation potential (E_0) was determined by the following equation; $E_0 = E_{peak} + \Delta E/2$, where E_{peak} is the potential of peak maximum and ΔE is the pulse amplitude. A. J. Bard and L. R. Faulkner, in *Electrochemical Methods-Fundamentals and Applications*, John Wiley & Sons, New York, 2nd edn, 2001, p. 290.

14 X. Wang, Y. Zhang, X. Sun, Y. Bian, C. Ma and J. Jiang, *Inorg. Chem.*, 2007, **46**, 7136.

15 P. V. Kamat, M. Haria and S. Hotchandani, *J. Phys. Chem. B*, 2004, **108**, 5166.

16 J. B. Foresman and A. Frisch, in *Exploring Chemistry with Electronic Structure Methods*, Gaussian Inc., Pittsburg, PA, 2nd edn, 1995, p. 62.

17 D. P. Hagberg, T. Edvinsson, T. Marinado, G. Boschloo, A. Hagfeldt and L. Sun, *Chem. Commun.*, 2006, 2245.

18 (*a*) H. Imahori, S. Hayashi, T. Umeyama, S. Eu, A. Oguro, S. Kang, Y. Matano, T. Shishido, S. Ngamsinlapasathian and S. Yoshikawa, *Langmuir*, 2006, **22**, 11405; (*b*) S. Eu, S. Hayashi, T. Umeyama, A. Oguro, M. Kawasaki, N. Kadota, Y. Matano and H. Imahori, *J. Phys. Chem. C*, 2007, **111**, 3528; (*c*) S. Eu, S. Hayashi, T. Umeyama, Y. Matano, Y. Araki and H. Imahori, *J. Phys. Chem. C*, 2008, **112**, 4396.

19 J. He, G. Benkö, F. Korodi, T. Polívka, R. Lomoth, B. Åkermark, L. Sun, A. Hagfeldt and V. Sundström, *J. Am. Chem. Soc.*, 2002, **124**, 4922.

20 The H_2Pc-sensitized TiO_2 cell displayed no photocurrent response, as predicted.

21 IPCE = LHE × ϕ_{inj} × η_{col}, where LHE is the light harvesting efficiency, ϕ_{inj} is the quantum yield of electron injection, and η_{col} is the efficiency of charge collection.

22 S. A. Haque, E. Palomares, B. M. Cho, A. N. M. Green, N. Hirata, D. R. Klug and J. R. Durrant, *J. Am. Chem. Soc.*, 2005, **127**, 3456.

23 S. N. Mori, W. Kubo, T. Kanzaki, N. Masaki, Y. Wada and S. Yanagida, *J. Phys. Chem. C*, 2007, **111**, 3522.

24 (*a*) A. N. M. Green, E. Palomares, S. A. Haque, J. M. Kroon and J. R. Durrant, *J. Phys. Chem. B*, 2005, **109**, 12525; (*b*) S. A. Haque, S. Handa, K. Peter, E. Palomares, M. Thelakkat and J. R. Durrant, *Angew. Chem., Int. Ed.*, 2005, **44**, 5740.

25 (*a*) B. O'Regan, J. E. Moser, M. Anderson and M. Grätzel, *J. Phys. Chem.*, 1990, **94**, 8720; (*b*) S. A. Haque, Y. Tachibana, D. R. Klug and J. R. Durrant, *J. Phys. Chem. B*, 1998, **102**, 1745; (*c*) T. A. Heimer, E. J. Heilweil, C. A. Bignozzi and G. J. Meyer, *J. Phys. Chem. A*, 2000, **104**, 4256; (*d*) J. N. Clifford, E. Palomares, Md. K. Nazeeruddin, M. Grätzel, J. Nelson, X. Li, N. J. Long and J. R. Durrant, *J. Am. Chem. Soc.*, 2004, **126**, 5225.

26 (*a*) G. Rothenberger, D. Fitzmaurice and M. Grätzel, *J. Phys. Chem. B*, 1992, **96**, 5983; (*b*) D. F. Watson, A. Marton, A. M. Stux and G. J. Meyer, *J. Phys. Chem. B*, 2003, **107**, 10971; (*c*) D. F. Watson, A. Marton, A. M. Stux and G. J. Meyer, *J. Phys. Chem. B*, 2004, **108**, 11680.

27 (*a*) P. Wang, S. M. Zakeeruddin, J. E. Moser, R. Humphry-Baker, P. Comte, V. Aranyos, A. Hagfeldt, Md. K. Nazeeruddin and M. Grätzel, *Adv. Mater.*, 2004, **16**, 1806; (*b*) A. Zaban, S. Ferrere, J. Sprague and B. Gregg, *J. Phys. Chem. B*, 1997, **101**, 55; (*c*) A. Zaban, S. Ferrere and B. Gregg, *J. Phys. Chem. B*, 1998, **102**, 452.

28 (*a*) M. Grätzel, *Pure Appl. Chem.*, 2001, **73**, 459; (*b*) Y. Tachibana, Md. K. Nazeeruddin, M. Grätzel, D. R. Klug and J. R. Durrant, *Chem. Phys.*, 2002, **285**, 127.

29 T. Sugimori, M. Torikata, J. Nojima, S. Tominaka, K. Tobikawa, M. Handa and K. Kasuga, *Inorg. Chem. Commun.*, 2002, **5**, 1031.

30 M. J. Frisch, G. W. Trucks, H. B. Schlegel, G. E. Scuseria, M. A. Robb, J. R. Cheeseman, J. A. Montgomery, Jr., T. Vreven, K. N. Kudin, J. C. Burant, J. M. Millam, S. S. Iyengar, J. Tomasi, V. Barone, B. Mennucci, M. Cossi, G. Scalmani, N. Rega, G. A. Petersson, H. Nakatsuji, M. Hada, M. Ehara, K. Toyota, R. Fukuda, J. Hasegawa, M. Ishida, T. Nakajima, Y. Honda, O. Kitao, H. Nakai, M. Klene, X. Li, J. E. Knox, H. P. Hratchian, J. B. Cross, V. Bakken, C. Adamo, J. Jaramillo, R. Gomperts, R. E. Stratmann, O. Yazyev, A. J. Austin, R. Cammi, C. Pomelli, J. Ochterski, P. Y. Ayala, K. Morokuma, G. A. Voth, P. Salvador, J. J. Dannenberg, V. G. Zakrzewski, S. Dapprich, A. D. Daniels, M. C. Strain, O. Farkas, D. K. Malick, A. D. Rabuck, K. Raghavachari, J. B. Foresman, J. V. Ortiz, Q. Cui, A. G. Baboul, S. Clifford, J. Cioslowski, B. B. Stefanov, G. Liu, A. Liashenko, P. Piskorz, I. Komaromi, R. L. Martin, D. J. Fox, T. Keith, M. A. Al-Laham, C. Y. Peng, A. Nanayakkara, M. Challacombe, P. M. W. Gill, B. G. Johnson, W. Chen, M. W. Wong, C. Gonzalez and J. A. Pople, *GAUSSIAN 03 (Revision C.02)*, Gaussian, Inc., Wallingford, CT, 2004.